Research Paper
Computational Methods for Differential Equations
http://cmde.tabrizu.ac.ir
Vol. *, No. *, *, pp. 1-22
DOI:10.22034/cmde.2025.63796.2861

Numerical Investigation of Smoking Behavior Dynamics Using Spectral Collocation Method

Keerthana G and Sagithya Thirumalai*
Department of Mathematics, School of Advanced Sciences, Vellore Institute of Technology, Chennai Campus, India.

Abstract

Smoking poses a significant threat to global public health and remains one of the leading causes of health problems. To examine these smoking-related issues, this paper aims to study the modified smoking model which represents a system of five-compartment such as potential smokers, snuffing class, irregular smokers, regular smokers, and quitters. A computational analysis was used to evaluate the model using the spectral collocation method. The core idea of the spectral collocation technique is to approximate the solution as a truncated series of basis functions using Chebyshev polynomials. By incorporating collocation points, the truncated series is transformed into an operational matrix form, which in turn converts the governing differential equations into a system of non-linear algebraic equations. Furthermore, the residual and absolute error for different collocation points is established. Additionally, the effects of various parameters such as transmission rate, recovery rate, quit rate, and death rate on the smoking model has been analyzed. All these computational investigations on the model are displayed in the form of figures. Finally, the effect of different combinations of parameters on the smoking dynamics and its impact is represented using contour plots.

Keywords. Smoking model, Spectral collocation method, Chebyshev polynomial.
2010 Mathematics Subject Classification. 92D25, 65M99, 33C99.

1. Introduction

Tobacco smoking is the foremost cause of preventable mortality. According to the WHO's report on the smoking epidemic [30], smoking claims the lives of many people during their most productive years. More than 5 million deaths worldwide are caused by the effects of smoking on various organs of the human body, and this number could increase up to 8 million annually by 2030 [16, 31]. Smokers have a 70 % higher risk of heart attack compared to non-smokers, and the incidence of lung cancer is 10 % higher among smokers. On average, smokers have 10 to 13 years shorter lifespans than non-smokers. Extensive medical records reveal that smoking tobacco is a primary contributor to a wide array of diseases, including lung cancer, heart attacks, strokes, respiratory illnesses, birth defects, and various other types of cancers and chronic conditions [23]. Additionally, tobacco kills an estimated 1.3 million non-smokers who are exposed to second-hand smoke annually [8]. The impact of smoking is profound, posing significant challenges both personally and socially. Therefore, understanding the dynamics of smoking is crucial to mitigate its associated risks. Mathematical modeling plays a pivotal role in understanding the spread of diseases and devising effective control strategies [1–3]. By leveraging mathematical models, researchers can analyze the intricate patterns of smoking behavior and its impact on health. To effectively illustrate the phenomenon of cigarette smoking, various researchers have explored numerous smoking models. These models help in identifying key factors that influence smoking initiation, continuation, and cessation.

Notably, in the year 1997, a simple mathematical model was introduced by Castillo-Garsow et al. [15] to study the dynamics of smoking. This initial study considered a smoking model with three compartments: potential smokers, regular smokers, and permanently quit smokers. In 2007, Ham [17] conducted a survey to collect data on various stages and methods of smoking among students in Korean schools. The following year, Sharomi and Gumel [22] developed

Received: 04 October 2024 ; Accepted: 22 May 2025.
* Corresponding author. Email: sagithya.t@vit.ac.in.

a mathematical model that introduced mild and chain smoker classes to analyse the progression of smoking-related illnesses. Building on the work of [15], Zaman [32] formulated an integer-order giving-up smoking model that included a light smoker class and demonstrated its qualitative behavior. This model was later extended to account for the possibility that once a smoker quits, they might become a potential smoker again [33].

In 2011, Choi et al. [10] developed a mathematical model to analyse adolescent nicotine dependence and smoking cessation dynamics. In 2013, Zaman [34] further advanced the field by introducing a novel smoking cessation square root model, which examines the finite-time extinction of smoking behavior using a non-standard finite difference (NSFD) scheme. In 2014, Alkhudhari et al. [4] expanded upon the system presented in [15, 22] and investigated the impact of smoking on quitters. In 2016, Din et al. [13] explored the qualitative behavior of a more complex smoking model with five compartments: non-smokers, smokers, temporary quitters, permanent quitters, and individuals with smoking-related illnesses. Mojeeb and Adu [21] examined the smoking epidemic through the counseling of smokers as an intervention. In 2018, Shah et al. [24] examined the tuberculosis caused by smoking. Later, in 2020 Ebraheem Alzahrani and Anwar Zeb [5] introduced a snuffing class to analyse tobacco smoking dynamics and develop control strategies using the NSFD scheme. In 2021, they proposed a smoking model with a reversion class and analysed it using NSFD method [36]. The square-root dynamics of the smoking model with cravings to smoke presented by Awan et al. [7] in 2021. Recently, various researchers have developed several smoking models to understand the dynamics of smoking in a better way. These efforts have expanded the field significantly, providing deeper insights into smoking behavior and potential intervention strategies [6, 11, 18–20, 29, 35].

In this study, we explore a non-linear smoking model with a unique snuffing class, inspired by the model presented in [5]. To achieve more accurate system dynamics, we include certain terms in the model that are not present in any other smoking models in the literature. That is, the quit rate and recovery rate for irregular smokers, and death due to smoking to the smoker classes such as irregular and regular smokers. These factors are critical for understanding the comprehensive impact of smoking and the potential for recovery and cessation. By incorporating these parameters, our model offers a deeper insight into the progression of smoking behaviors and the effectiveness of intervention strategies, ultimately contributing to a more precise analysis of the smoking epidemic.

In literature, researchers have typically relied on standard numerical techniques to solve smoking dynamic models. Spectral collocation [14, 25–28] is one of the such emerging numerical techniques to solve mathematical models. In this method, the approximate solution are represented as truncated series of global basis functions. In this research paper, we employ the prevailing spectral collocation method using Chebyshev polynomial [9, 12] as a basis function. This approach offers distinct advantages over traditional methods due to the global nature of its basis functions. The spectral collocation method provides higher accuracy and efficiency, allowing for precise modeling of complex interactions within the smoking population. Additionally, its exponential convergence and reduced computational time make it a more powerful numerical technique. To efficiently solve the system of equations, we employ the spectral collocation method, a technique that has not been attempted in the literature.

The rest of the paper is structured as follows: In section 2, we present the details of smoking model. In section 3 the author describes the key higlights and the mathematical procedure of the spectral approach of solution and presents the numerical results of the model in section 4. This section also includes a detailed representation of the effects of various parameters with figures that support our discussions. Finally, the overall conclusions are provided in section 5.

2. Model formulation

In this section, a modified smoking model is formulated by considering various influencing parameters to frame the new model. The whole population (M) is split up into five compartments, which are as follows:

(i) **Potential smokers** (P) are current non-smokers and they are vulnerable and may smoke in the future.
(ii) **Snuffing class** (I) refers to individuals who inhale tobacco through their nostrils.
(iii) **Irregular smokers** (S_I) are those who exhibit inconsistent smoking habits.
(iv) **Regular smokers** (S_R) are those who smoke consistently.
(v) **Quit smokers** (Q) are individuals who have stopped smoking.

Let the population have a constant birth rate b. Initially, individuals in the potential smokers class can be transmitted to the snuffing class at a transmission rate l_1 due to inhaling tobacco through the nostrils. In the snuffing class, individuals may die due to snuffing at a rate σ_1. The transmission of individuals from the snuffing class to the irregular smokers occurs at a rate of l_2, while others move to regular smokers at a rate l_3. Regular smokers can recover and revert to the potential smokers class at a recovery rate γ_2 or they may quit smoking and join the quitters at a quit rate α_2. The population experiences natural death at a rate β.

In view of above said idea, the author has introduced the parameters such as the recovery rate (γ_1) and quit rate (α_1) for irregular smokers, and the death rate due to smoking (σ_2, σ_3) for both irregular and regular smokers. That is, irregular smokers can recover and revert to the potential smokers class at a recovery rate, or they may quit smoking and join the quitters at a quit rate. Individuals in the irregular and regular smokers classes may also die due to smoking respectively. Considering all the parameters, governing the smoking model are formulated into a system of first-order differential equations with five compartments as follows:

$$\frac{dP}{dt} = b - l_1PI - \beta P + \gamma_1 S_I + \gamma_2 S_R, \tag{2.1}$$

$$\frac{dI}{dt} = l_1PI - l_2IS_I - (\sigma_1 + \beta)I, \tag{2.2}$$

$$\frac{dS_I}{dt} = l_2IS_I - (l_3 + \sigma_2 + \beta + \gamma_1 + \alpha_1)S_I, \tag{2.3}$$

$$\frac{dS_R}{dt} = l_3S_I - (\alpha_2 + \beta + \gamma_2 + \sigma_3)S_R, \tag{2.4}$$

$$\frac{dQ}{dt} = \alpha_1 S_I - \beta Q + \alpha_2 S_R. \tag{2.5}$$

with the initial conditions $P(0) \geq 0$, $I(0) \geq 0$, $S_I(0) \geq 0$, $S_R(0) \geq 0$, $Q(0) \geq 0$, where the list of parameters used are tabulated in Table 1.

Table 1. Model parameters and values with their descriptions.

Parameters	Description	Parameter values	Source
b	Birth rate	0.1	[22]
l_1	Transmission rate between susceptible and snuffing	0.003	[22]
l_2	Transmission rate between snuffing and irregular	0.002	[22]
l_3	Transmission rate between irregular and regular	0.05	[29]
α_1	Quit rate for irregular smokers	0.05	[22]
α_2	Quit rate for regular smokers	0.05	[22]
β	Natural death rate	0.002	[22]
γ_1	Recovery rate for irregular smoking	0.001	[22]
γ_2	Recovery rate for regular smoking	0.001	[22]
σ_1	Death due to snuffing	0.003	[22]
σ_2	Death due to irregular smoking	0.003	[22]
σ_3	Death due to regular smoking	0.003	[22]

3. Key highlights and methodology of the present study

In this paper, we consider a modified five-compartment smoking model, formulated as a system of nonlinear differential equations. This model incorporates three additional parameters: the recovery rate (γ_1) and quit rate (α_1) for irregular smokers, as well as the death rates due to smoking (σ_2, σ_3) for irregular and regular smokers respectively.

To analyze this model numerically, we employ the spectral collocation method using Chebyshev polynomials as the basis function. The spectral collocation method is one of the most widely used techniques for solving differential equations. Its fundamental idea is to express the approximate solution of the differential equation by a truncated series of basis function. This method is computationally efficient, exhibit rapid convergence and provide high accuracy, particularly as the number of collocation points increases. One of the primary advantages of spectral methods is their exponential convergence rate for infinitely differentiable basis functions, making them highly effective for solving complex differential equations. The computational procedure is represented in Figure 1.

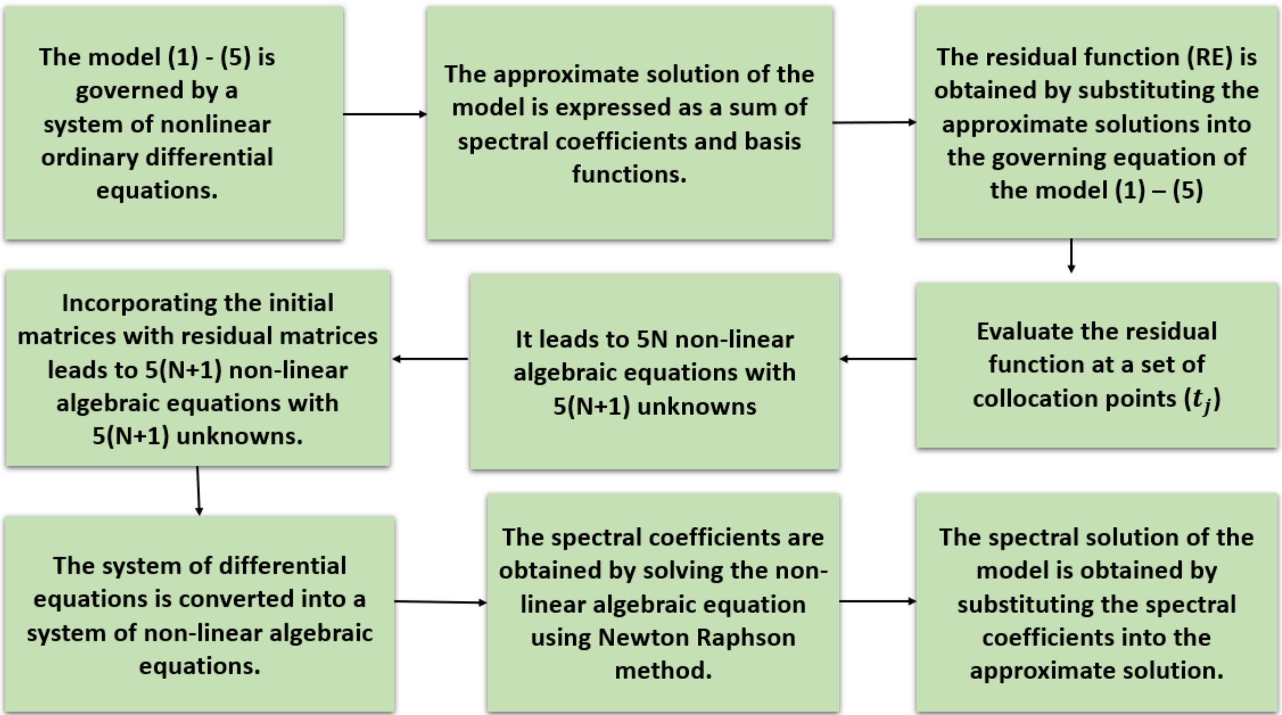

FIGURE 1. Graphical illustration of the spectral collocation method.

3.1. **Present analysis.** In this section, the solutions of the governing Equations (2.1) - (2.5) which is a system of first order differential equations is evaluated using Chebyshev spectral Collocation method over the time interval $[0, L]$.

Let us consider the spectral solution for $[0, L]$ is of the form

$$\mathbf{P(t)} \approx \mathbf{P_N(t)} = \sum_{i=0}^{N} p_i \psi_i \left(\frac{2t - L}{L} \right) \tag{3.1}$$

$$\mathbf{I(t)} \approx \mathbf{I_N(t)} = \sum_{i=0}^{N} e_i \psi_i \left(\frac{2t - L}{L} \right) \tag{3.2}$$

$$\mathbf{S_I(t)} \approx \mathbf{S_{I_N(t)}} = \sum_{i=0}^{N} c_i \psi_i \left(\frac{2t - L}{L} \right) \tag{3.3}$$

$$\mathbf{S_R(t)} \approx \mathbf{S_{R_N(t)}} = \sum_{i=0}^{N} d_i \psi_i \left(\frac{2t - L}{L} \right) \tag{3.4}$$

$$\mathbf{Q(t)} \approx \mathbf{Q_N(t)} = \sum_{i=0}^{N} q_i \psi_i \left(\frac{2t - L}{L} \right) \tag{3.5}$$

where $\psi_i\left(\frac{2t-L}{L}\right)$ denotes the set of shifted Chebyshev polynomial, N represents the number of collocation points and $p_i's, e_i's, c_i's, d_i's, q_i's$ are the spectral coefficients. On substituting the spectral solutions (3.1) - (3.5) in (2.1) - (2.5), yields the residual functions given by

$$\mathbf{RE_{1,N}(t)} := b - l_1\mathbf{P_N(t)I_N(t)} - \beta\mathbf{P_N(t)} + \gamma_1\mathbf{S_{I_N}(t)} + \gamma_2\mathbf{S_{R_N}(t)} - \frac{\mathbf{dP_N(t)}}{\mathbf{dt}}, \tag{3.6}$$

$$\mathbf{RE_{2,N}(t)} := l_1\mathbf{P_N(t)I_N(t)} - l_2\mathbf{I_N(t)S_{I_N}(t)} - (\sigma_1+\beta)\mathbf{I_N(t)} - \frac{\mathbf{dI_N(t)}}{\mathbf{dt}}, \tag{3.7}$$

$$\mathbf{RE_{3,N}(t)} := l_2\mathbf{I_N(t)S_{I_N}(t)} - (l_3+\sigma_2+\beta+\gamma_1+\alpha_1)\mathbf{S_{I_N}(t)} - \frac{\mathbf{dS_{I_N}(t)}}{\mathbf{dt}}, \tag{3.8}$$

$$\mathbf{RE_{4,N}(t)} := l_3\mathbf{S_{I_N}(t)} - (\alpha_2+\beta+\gamma_2+\sigma_3)\mathbf{S_{R_N}(t)} - \frac{\mathbf{dS_{R_N}(t)}}{\mathbf{dt}}, \tag{3.9}$$

$$\mathbf{RE_{5,N}(t)} := \alpha_1\mathbf{S_{I_N}(t)} - \beta\mathbf{Q_N(t)} + \alpha_2\mathbf{S_{R_N}(t)} - \frac{\mathbf{dQ_N(t)}}{\mathbf{dt}}. \tag{3.10}$$

The core idea of the proposed method is to enforce the residual function to be zero at a set of collocation points t_j, where j ranges from 1 to $N-1$. Thus, the residual function (3.6) – (3.10) becomes

$$\mathbf{RE_{1,N}}(t_j) := b - l_1\mathbf{P_N}(t_j)\mathbf{I_N}(t_j) - \beta\mathbf{P_N}(t_j) + \gamma_1\mathbf{S_{I_N}}(t_j) + \gamma_2\mathbf{S_{R_N}}(t_j) - \frac{d\mathbf{P_N}(t_j)}{dt} = 0, \tag{3.11}$$

$$\mathbf{RE_{2,N}}(t_j) := l_1\mathbf{P_N}(t_j)\mathbf{I_N}(t_j) - l_2\mathbf{I_N}(t_j)\mathbf{S_{I_N}}(t_j) - (\sigma_1+\beta)\mathbf{I_N}(t_j) - \frac{d\mathbf{I_N}(t_j)}{dt} = 0, \tag{3.12}$$

$$\mathbf{RE_{3,N}}(t_j) := l_2\mathbf{I_N}(t_j)\mathbf{S_{I_N}}(t_j) - (l_3+\sigma_2+\beta+\gamma_1+\alpha_1)\mathbf{S_{I_N}}(t_j) - \frac{d\mathbf{S_{I_N}}(t_j)}{dt} = 0, \tag{3.13}$$

$$\mathbf{RE_{4,N}}(t_j) := l_3\mathbf{S_{I_N}}(t_j) - (\alpha_2+\beta+\gamma_2+\sigma_3)\mathbf{S_{R_N}}(t_j) - \frac{d\mathbf{S_{R_N}}(t_j)}{dt} = 0, \tag{3.14}$$

$$\mathbf{RE_{5,N}}(t_j) := \alpha_1\mathbf{S_{I_N}}(t_j) - \beta\mathbf{Q_N}(t_j) + \alpha_2\mathbf{S_{R_N}}(t_j) - \frac{d\mathbf{Q_N}(t_j)}{dt} = 0. \tag{3.15}$$

The collocation points will differ depending on the choice of basis function. In this study, we use Chebyshev polynomials, for which the collocation points are defined as follows:

$$t_j = \frac{L}{2}\left(1 - \cos\frac{j\pi}{N}\right).$$

When using Legendre and Jacobi polynomials as basis functions, the collocation points are determined by the zeros of their first derivatives.

On substituting the selected basis functions and collocation points in (3.1) - (3.5), we get

$$\mathbf{P(t_j)} \approx \mathbf{P_N(t_j)} = \mathbf{D_jP}, \tag{3.16}$$

$$\mathbf{I(t_j)} \approx \mathbf{I_N(t_j)} = \mathbf{D_jI}, \tag{3.17}$$

$$\mathbf{S_I(t_j)} \approx \mathbf{S_{I_N}(t_j)} = \mathbf{D_jS_I}, \tag{3.18}$$

$$\mathbf{S_R(t_j)} \approx \mathbf{S_{R_N}(t_j)} = \mathbf{D_jS_R}, \tag{3.19}$$

$$\mathbf{Q(t_j)} \approx \mathbf{Q_N(t_j)} = \mathbf{D_jQ}, \tag{3.20}$$

where

$$\mathbf{D_j} = \begin{bmatrix}\psi_0(t_j) & \psi_1(t_j) & \dots & \psi_N(t_j)\end{bmatrix}_{1\times N+1}, \tag{3.21}$$

$$\mathbf{P} = \begin{bmatrix} p_0 \\ p_1 \\ \vdots \\ p_N \end{bmatrix}_{N+1\times 1}, \quad \mathbf{I} = \begin{bmatrix} e_0 \\ e_1 \\ \vdots \\ e_N \end{bmatrix}_{N+1\times 1}, \quad \mathbf{S_I} = \begin{bmatrix} c_0 \\ c_1 \\ \vdots \\ c_N \end{bmatrix}_{N+1\times 1}, \quad \mathbf{S_R} = \begin{bmatrix} d_0 \\ d_1 \\ \vdots \\ d_N \end{bmatrix}_{N+1\times 1}, \quad \mathbf{Q} = \begin{bmatrix} q_0 \\ q_1 \\ \vdots \\ q_N \end{bmatrix}_{N+1\times 1}, \tag{3.22}$$

where $\mathbf{P}, \mathbf{I}, \mathbf{S_I}, \mathbf{S_R}$ and $\mathbf{Q}$ are the coefficient matrix of the system (3.1)–(3.5). In order to rewrite the above residual functions (3.11)–(3.15) in a more simplified form. Let us introduce the matrices as follows:

$$\mathbf{D} = \begin{bmatrix} \mathbf{D_1} \\ \mathbf{D_2} \\ \vdots \\ \mathbf{D_N} \end{bmatrix}_{N\times 1} = \begin{bmatrix} \psi_0(t_1) & \psi_1(t_1) & \dots & \psi_N(t_1) \\ \psi_0(t_2) & \psi_1(t_2) & \dots & \psi_N(t_2) \\ \vdots & \vdots & \dots & \vdots \\ \psi_0(t_N) & \psi_1(t_N) & \dots & \psi_N(t_N) \end{bmatrix}_{N\times N+1}, \tag{3.23}$$

$$\mathbf{D^{(1)}} = \begin{bmatrix} \mathbf{D_1^{(1)}} \\ \mathbf{D_2^{(1)}} \\ \vdots \\ \mathbf{D_N^{(1)}} \end{bmatrix}_{N\times 1} = \begin{bmatrix} \psi_0^{(1)}(t_1) & \psi_1^{(1)}(t_1) & \dots & \psi_N^{(1)}(t_1) \\ \psi_0^{(1)}(t_2) & \psi_1^{(1)}(t_2) & \dots & \phi_N^{(1)}(t_2) \\ \vdots & \vdots & \dots & \vdots \\ \psi_0^{(1)}(t_N) & \psi_1^{(1)}(t_N) & \dots & \psi_N^{(1)}(t_N) \end{bmatrix}_{N\times N+1}, \tag{3.24}$$

where $\mathbf{D}$ denotes the basis matrix and $\mathbf{D^{(1)}}$ denotes the basis matrix for the first order differentiation. The residual function is rewritten as follows:

$$\mathbf{RE_1} = \begin{bmatrix} \mathbf{RE_{1,N}(t_1)} \\ \mathbf{RE_{1,N}(t_2)} \\ \vdots \\ \mathbf{RE_{1,N}(t_N)}) \end{bmatrix}_{N\times 1}, \quad \mathbf{RE_2} = \begin{bmatrix} \mathbf{RE_{2,N}(t_1)} \\ \mathbf{RE_{2,N}(t_2)} \\ \vdots \\ \mathbf{RE_{2,N}(t_N)}) \end{bmatrix}_{N\times 1}, \quad \mathbf{RE_3} = \begin{bmatrix} \mathbf{RE_{3,N}(t_1)} \\ \mathbf{RE_{3,N}(t_2)} \\ \vdots \\ \mathbf{RE_{3,N}(t_N)}) \end{bmatrix}_{N\times 1}, \tag{3.25}$$

$$\mathbf{RE_4} = \begin{bmatrix} \mathbf{RE_{4,N}(t_1)} \\ \mathbf{RE_{4,N}(t_2)} \\ \vdots \\ \mathbf{RE_{4,N}(t_N)}) \end{bmatrix}_{N\times 1}, \quad \mathbf{RE_5} = \begin{bmatrix} \mathbf{RE_{5,N}(t_1)} \\ \mathbf{RE_{5,N}(t_2)} \\ \vdots \\ \mathbf{RE_{5,N}(t_N)}) \end{bmatrix}_{N\times 1}, \tag{3.26}$$

where $\mathbf{RE_1}, \mathbf{RE_2}, \mathbf{RE_3}$, $\mathbf{RE_4}$ and $\mathbf{RE_5}$ are the residual matrices for the system (2.1)–(2.5). On substituting the above matrices (3.21)–(3.26) into (3.11)–(3.15) the residual function reduces to

$$\mathbf{RE_1} := b\mathbf{E} - l_1\mathbf{DPDI} - \beta\mathbf{DP} + \gamma_1\mathbf{DS_I} + \gamma_2\mathbf{DS_R} - \mathbf{D^{(1)}P} = [\mathbf{0}], \tag{3.27}$$

$$\mathbf{RE_2} := l_1\mathbf{DPDI} - l_2\mathbf{DIDS_I} - (\sigma_1+\beta)\mathbf{DI} - \mathbf{D^{(1)}I} = [\mathbf{0}], \tag{3.28}$$

$$\mathbf{RE_3} := l_2\mathbf{DIDS_I} - (l_3+\sigma_2+\beta+\gamma_1+\alpha_1)\mathbf{DS_I(t)} - \mathbf{D^{(1)}S_I} = [\mathbf{0}], \tag{3.29}$$

$$\mathbf{RE_4} := l_3\mathbf{DS_I} - (\alpha_2+\beta+\gamma_2+\sigma_3)\mathbf{DS_R} - \mathbf{D^{(1)}S_R} = [\mathbf{0}], \tag{3.30}$$

$$\mathbf{RE_5} := \alpha_1\mathbf{DS_I} - \beta\mathbf{DQ} + \alpha_2\mathbf{DS_R} - \mathbf{D^{(1)}Q} = [\mathbf{0}]. \tag{3.31}$$

where $\mathbf{E}$ is a column matrix of order $N\times 1$ with unit entries. Introducing the matrices $\mathbf{Y_1}$ and $\mathbf{Y_2}$ of the form,

$$\mathbf{Y_1} = \begin{bmatrix} \mathbf{(DP)_1} & 0 & \dots & 0 \\ 0 & \mathbf{(DP)_2} & \dots & 0 \\ \vdots & \vdots & \dots & \vdots \\ 0 & 0 & \dots & \mathbf{(DP)_N} \end{bmatrix}_{N\times N}, \quad \mathbf{Y_2} = \begin{bmatrix} \mathbf{(DS_I)_1} & 0 & \dots & 0 \\ 0 & \mathbf{(DS_I)_2} & \dots & 0 \\ \vdots & \vdots & \dots & \vdots \\ 0 & 0 & \dots & \mathbf{(DS_I)_N} \end{bmatrix}_{N\times N}, \tag{3.32}$$

where $\mathbf{(DP)_i}$ is the i^{th} row vector of the matrix $\mathbf{DP}$. Similarly, $\mathbf{(DS_I)_i}$ is the i^{th} row vector of the matrix $\mathbf{DS_I}$. Substituting (3.32) into the system (3.27)–(3.31), we obtain:

$$\mathbf{RE_1} := b\mathbf{E} - l_1\mathbf{Y_1DI} - \beta\mathbf{DP} + \gamma_1\mathbf{DS_I} + \gamma_2\mathbf{DS_R} - \mathbf{D^{(1)}P} = [\mathbf{0}], \tag{3.33}$$

$$\mathbf{RE_2} := l_1\mathbf{Y_1DI} - l_2\mathbf{DIY_2} - (\sigma_1+\beta)\mathbf{DI} - \mathbf{D^{(1)}I} = [\mathbf{0}], \tag{3.34}$$

$$\mathbf{RE_3} := l_2\mathbf{DIY_2} - (l_3+\sigma_2+\beta+\gamma_1+\alpha_1)\mathbf{DS_I(t)} - \mathbf{D^{(1)}S_I} = [\mathbf{0}], \tag{3.35}$$

$$\mathbf{RE_4} := l_3\mathbf{DS_I} - (\alpha_2+\beta+\gamma_2+\sigma_3)\mathbf{DS_R} - \mathbf{D^{(1)}S_R} = [\mathbf{0}], \tag{3.36}$$

$$\mathbf{RE_5} := \alpha_1 \mathbf{DS_I} - \beta \mathbf{DQ} + \alpha_2 \mathbf{DS_R} - \mathbf{D^{(1)}Q} = [\mathbf{0}]. \tag{3.37}$$

The residual matrices in (3.33)–(3.37) result in $5N$ nonlinear algebraic equations with $5(N+1)$ unknowns. By incorporating the spectral solution into the five initial conditions, we obtain a simplified matrix form of the initial condition as follows:

$$\mathbf{D_0P} = u_1, \mathbf{D_0I} = u_2, \mathbf{D_0S_I} = u_3, \mathbf{D_0S_R} = u_4, \mathbf{D_0Q} = u_5, \tag{3.38}$$

where

$$\mathbf{D_0} = \begin{bmatrix} \psi_0(0) & \psi_1(0) & \dots & \psi_N(0) \end{bmatrix}_{1\times N+1}. \tag{3.39}$$

On incorporating the initial matrices (3.38) with the residual matrices (3.33)–(3.37), we have a system of $5(N+1)$ nonlinear algebraic equations with $5(N+1)$ unknowns, which is represented by the following reduced matrix system:

$$\begin{bmatrix} \mathbf{RE_{1,N}} \\ \mathbf{RE_{2,N}} \\ \mathbf{RE_{3,N}} \\ \mathbf{RE_{4,N}} \\ \mathbf{RE_{5,N}} \\ \mathbf{D_0P} \\ \mathbf{D_0I} \\ \mathbf{D_0S_I} \\ \mathbf{D_0S_R} \\ \mathbf{D_0Q} \end{bmatrix} = \begin{bmatrix} 0 \\ 0 \\ 0 \\ 0 \\ 0 \\ u_1 \\ u_2 \\ u_3 \\ u_4 \\ u_5 \end{bmatrix}. \tag{3.40}$$

The spectral coefficients p_i', e_i', c_i', d_i', and q_i' are obtained by solving the system of nonlinear algebraic equations (3.40) using the Newton-Raphson method. By substituting the spectral coefficients into Equation (3.1)–(3.5), we derive the spectral solutions $P(t), I(t), S_I(t), S_R(t)$ and $Q(t)$.

In addition,

- Spectral solutions obtained are compared with fourth order Runge Kutta method (RK4) to analyse and present the absolute errors for different values of N to show the good accuracy of the present method and also to examine the residual error for different values of N which helps to assess the accuracy and convergence of the proposed computational method.
- The effect of distinct parameters such as transmission rates, death rates by smoking/snuffing, recovery rate, natural death rate, and quit rate on the five different compartments of the smoking model is investigated.
- The combined effect of three transmission rates, transmission and recovery rate, as well as the transmission and quit rate, transmission and death rate on the system dynamics is analyzed, in order to understand the combined effects of different parameters simultaneously.

In the next section, we implement this approach to the model using Chebyshev polynomials as the basis function and provide the computational implementation along with the results obtained from this method.

4. Numerical results

In this section, we present the computations and results obtained for the smoking model (2.1)–(2.5) using spectral collocation method with Chebyshev polynomials as basis function. The set of parameter values considered for the study are $b = 0.1$, $l_1 = 0.003$, $l_2 = 0.002$, $l_3 = 0.05$, $\beta = 0.002$, $\gamma_1 = \gamma_2 = 0.001$, $\sigma_1 = \sigma_2 = \sigma_3 = 0.003$, $\alpha_1 = \alpha_2 = 0.05$ with initial conditions $S(0) = 40$, $I(0) = 30$, $S_I(0) = 20$, $S_R(0) = 10$, $Q(0) = 5$ [29].

As an illustration, we have applied the spectral collocation method for the governing model (2.1)–(2.5) by considering the Chebyshev polynomial (T_i) as a basis function for N = 7 in [0,50]. The spectral solution for the smoking model is presented as follows:

$$\mathbf{P(t)} \approx \mathbf{P_7(t)} = \sum_{i=0}^{7} p_i \psi_i \left(\frac{2t-50}{50} \right) = \sum_{i=0}^{7} p_i T_i \left(\frac{t-25}{25} \right), \tag{4.1}$$

$$\mathbf{I(t)} \approx \mathbf{I_7(t)} = \sum_{i=0}^{7} e_i \psi_i \left(\frac{2t-50}{50}\right) = \sum_{i=0}^{7} e_i T_i \left(\frac{t-25}{25}\right), \tag{4.2}$$

$$\mathbf{S_I(t)} \approx \mathbf{S_{I_7(t)}} = \sum_{i=0}^{7} c_i \psi_i \left(\frac{2t-50}{50}\right) = \sum_{i=0}^{7} c_i T_i \left(\frac{t-25}{25}\right), \tag{4.3}$$

$$\mathbf{S_R(t)} \approx \mathbf{S_{R_7(t)}} = \sum_{i=0}^{7} d_i \psi_i \left(\frac{2t-50}{50}\right) = \sum_{i=0}^{7} d_i T_i \left(\frac{t-25}{25}\right), \tag{4.4}$$

$$\mathbf{Q(t)} \approx \mathbf{Q_7(t)} = \sum_{i=0}^{7} q_i \psi_i \left(\frac{2t-50}{50}\right) = \sum_{i=0}^{7} q_i T_i \left(\frac{t-25}{25}\right). \tag{4.5}$$

The residual functions which takes the form (3.6)–(3.10) are considered to be zero at a set of seven collocation points as N = 7. The collocation points for shifted Chebyshev polynomial basis functions are calculated using $t_j = 25\left(1-\cos\dfrac{\pi j}{7}\right)$ as $t_0 = 0$, $t_1 = 2.4758$, $t_2 = 9.4128$, $t_3 = 19.4370$, $t_4 = 30.5630$, $t_5 = 40.5872$, $t_6 = 47.5242$, $t_7 = 50.0000$.
Substituting the above collocation points in Chebyshev polynomials gives the basis matrix $\mathbf{D}$ and first order differentiation matrix $\mathbf{D^{(1)}}$ as follows:

$$\mathbf{D} = \begin{bmatrix} 1.00000 & -1.00000 & 1.00000 & -1.00000 & 1.00000 & -1.00000 & 1.00000 & -1.00000 \\ 1.00000 & -0.90097 & 0.62349 & -0.22252 & -0.22253 & 0.62350 & -0.90097 & 1.00000 \\ 1.00000 & -0.62349 & -0.22253 & 0.90097 & -0.90096 & 0.22251 & 0.62350 & -1.00000 \\ 1.00000 & -0.22252 & -0.90097 & 0.62349 & 0.62349 & -0.90097 & -0.22253 & 1.00000 \\ 1.00000 & 0.22252 & -0.90097 & -0.62349 & 0.62349 & 0.90097 & -0.22253 & -1.00000 \\ 1.00000 & 0.62349 & -0.22253 & -0.90097 & -0.90096 & -0.22251 & 0.62350 & 1.00000 \\ 1.00000 & 0.90097 & 0.62349 & 0.22252 & -0.22253 & -0.62350 & -0.90097 & -1.00000 \\ 1.00000 & 1.00000 & 1.00000 & 1.00000 & 1.00000 & 1.00000 & 1.00000 & 1.00000 \end{bmatrix}_{8\times 8} \tag{4.6}$$

$$\mathbf{D^{(1)}} = \begin{bmatrix} 0.00000 & 0.04000 & -0.16000 & 0.36000 & -0.64000 & 1.00000 & -1.44000 & 1.96000 \\ 0.00000 & 0.04000 & -0.14415 & 0.26964 & -0.35951 & 0.36038 & -0.23999 & -0.00001 \\ 0.00000 & 0.04000 & -0.09976 & 0.06659 & 0.08879 & -0.24940 & 0.24000 & 0.00001 \\ 0.00000 & 0.04000 & -0.03560 & -0.09623 & 0.12831 & 0.08901 & -0.24000 & -0.00000 \\ 0.00000 & 0.04000 & 0.03560 & -0.09623 & -0.12831 & 0.08901 & 0.24000 & -0.00000 \\ 0.00000 & 0.04000 & 0.09976 & 0.06659 & -0.08879 & -0.24940 & -0.24000 & 0.00001 \\ 0.00000 & 0.04000 & 0.14415 & 0.26964 & 0.35951 & 0.36038 & 0.23999 & -0.00001 \\ 0.00000 & 0.04000 & 0.16000 & 0.36000 & 0.64000 & 1.00000 & 1.44000 & 1.96000 \end{bmatrix}_{8\times 8} \tag{4.7}$$

The coefficient matrices are given by:

$$\mathbf{P} = \begin{bmatrix} p_0 \\ p_1 \\ p_2 \\ \vdots \\ p_7 \end{bmatrix}_{8\times 1}, \mathbf{I} = \begin{bmatrix} e_0 \\ e_1 \\ e_2 \\ \vdots \\ e_7 \end{bmatrix}_{8\times 1}, \mathbf{S_I} = \begin{bmatrix} c_0 \\ c_1 \\ c_2 \\ \vdots \\ c_7 \end{bmatrix}_{8\times 1}, \mathbf{S_R} = \begin{bmatrix} d_0 \\ d_1 \\ d_2 \\ \vdots \\ d_7 \end{bmatrix}_{8\times 1}, \quad \mathbf{Q} = \begin{bmatrix} q_0 \\ q_1 \\ q_2 \\ \vdots \\ q_7 \end{bmatrix}_{8\times 1}. \tag{4.8}$$

$$\mathbf{Y_1} = \begin{bmatrix} (\mathbf{DP})_\mathbf{1} & 0 & \dots & 0 \\ 0 & (\mathbf{DP})_\mathbf{2} & \dots & 0 \\ \vdots & \vdots & \dots & \vdots \\ 0 & 0 & \dots & (\mathbf{DP})_\mathbf{7} \end{bmatrix}_{7\times 7}, \quad \mathbf{Y_2} = \begin{bmatrix} (\mathbf{DS_I})_\mathbf{1} & 0 & \dots & 0 \\ 0 & (\mathbf{DS_I})_\mathbf{2} & \dots & 0 \\ \vdots & \vdots & \dots & \vdots \\ 0 & 0 & \dots & (\mathbf{DS_I})_\mathbf{7} \end{bmatrix}_{7\times 7}, \tag{4.9}$$

On incorporating all these matrices, the residual functions reduces to

$$\mathbf{RE_{1,7}(t)} := 0.1\mathbf{E} - 0.003\mathbf{Y_1DI} - 0.002\mathbf{DP} + 0.001\mathbf{DS_I} + 0.001\mathbf{DS_R} - \mathbf{D^{(1)}P} = [\mathbf{0}], \tag{4.10}$$

$$\mathbf{RE_{2,7}(t)} := 0.003\mathbf{Y_1DI} - 0.002\mathbf{DIY_2} - (0.003 + 0.002)\mathbf{DI} - \mathbf{D^{(1)}I} = [\mathbf{0}], \tag{4.11}$$

$$\mathbf{RE_{3,7}(t)} := 0.002\mathbf{DIY_2} - (0.05 + 0.003 + 0.002 + 0.001 + 0.05)\mathbf{DS_I} - \mathbf{D^{(1)}S_I} = [\mathbf{0}], \tag{4.12}$$

$$\mathbf{RE_{4,7}(t)} := 0.05\mathbf{DS_I} - (0.05 + 0.002 + 0.001 + 0.003)\mathbf{DS_R} - \mathbf{D^{(1)}S_R} = [\mathbf{0}], \tag{4.13}$$

$$\mathbf{RE_{5,7}(t)} := 0.05\mathbf{DS_R} - 0.002\mathbf{DQ} + 0.05\mathbf{DS_I} - \mathbf{D^{(1)}Q} = [\mathbf{0}]. \tag{4.14}$$

Thus, the residual matrices (4.10)–(4.14) have a set of 35 non-linear algebraic equations with 40 unknowns. On adding the initial condition matrices such as

$$\mathbf{D_0P} = 40, \mathbf{D_0I} = 30, \mathbf{D_0S_I} = 20, \mathbf{D_0S_R} = 10, \mathbf{D_0Q} = 5, \tag{4.15}$$

where

$$\mathbf{D_0} = \begin{bmatrix} 1 & -1 & 1 & -1 & 1 & -1 & 1 & -1 \end{bmatrix}, \tag{4.16}$$

into the system (4.10)–(4.14), we obtain a system of 40 non-linear algebraic equations with 40 unknowns. On solving these equations using Newtons method yields the spectral coefficients which on substituting to governing equations gives the spectral solution as follows:

$$\begin{aligned}
\mathbf{P_7(t)} &= -3.550000001t + 1.849668996 \times 10^{-9}t^7 - 3.352585862 \times 10^{-7}t^6 + 0.00002400863571t^5 \\
&\quad - 0.0008389319585t^4 + 0.01298069004t^3 + 0.02021003456t^2 + 40.00000000, \\
\mathbf{I_7(t)} &= 2.250000000t + 30.00000000 - 2.044452954 \times 10^{-9}t^7 + 3.671125036 \times 10^{-7}t^6 \\
&\quad - 0.00002581972505t^5 + 0.0008677869265t^4 - 0.01207075497t^3 - 0.04042766470t^2, \\
\mathbf{S_{I_7}(t)} &= -0.9200000001t + 20.00000000 + 9.187892770 \times 10^{-11}t^7 - 8.745394337 \times 10^{-9}t^6 \\
&\quad - 2.85196134 \times 10^{-7}t^5 + 0.00006705089836t^4 - 0.003219790880t^3 + 0.06670334130t^2, \\
\mathbf{S_{R_7}(t)} &= 0.4400000001t + 9.999999999 + 7.520085458 \times 10^{-11}t^7 - 1.618341182 \times 10^{-8}t^6 \\
&\quad + 1.420569002 \times 10^{-6}t^5 - 0.00006536795853t^4 + 0.001773304480t^3 - 0.03532510961t^2, \\
\mathbf{Q_7(t)} &= 1.490000001t + 4.999999999 + 1.634965754 \times 10^{-12}t^7 - 2.638623177 \times 10^{-9}t^6 \\
&\quad + 4.181869371 \times 10^{-7}t^5 - 0.00002479296381t^4 + 0.0005796093071t^3 - 0.01360149555t^2.
\end{aligned} \tag{4.17}$$

Residual error for various values of N in $[0, 20]$ is represented in Figure 2. It is observed from the figure that, as N increases, the residual error decreases. It can be noticed that as N increases from 5 to 20, the maximum residual error for $P(t)$, $I(t)$ decreases from $O(10^{-1})$ to $O(10^{-5})$ and $S_I(t)$ decreases from $O(10^{-1})$ to $O(10^{-6})$. Similarly, the residual error for $S_R(t)$ and $Q(t)$ decreases from $O(10^{-1})$ to $O(10^{-7})$, as shown in Figure 2(d)–2(e). Thus, Figure 2 demonstrates that the residual error converges as N increases.

Figure 3 illustrates the absolute error between the present method and RK4 for different values of N. The figure demonstrates that as N increases, the error decreases, suggesting that larger values of N lead to more accurate solution. As N increases from 7 to 15, the absolute error decreases from $O(10^{-2})$ to $O(10^{-5})$ for $P(t)$, from $O(10^{-1})$ to $O(10^{-5})$ for $I(t)$, from $O(10^{-3})$ to $O(10^{-6})$ for $S_I(t)$, and from $O(10^{-3})$ to $O(10^{-7})$ for both $S_R(t)$ and $Q(t)$. It is observed from the figure that as N increases, the absolute error decreases. Figure 4–10 depicts the potential effects of various parameters influencing the current smoking model. Figure 4 illustrates the dynamics of the system with the snuffing/smoking-related death rates (σ) over the snuffing, irregular, and regular smoker categories. When snuffing / smoking-related death occurs, the population size of smokers decreases as shown in Figure 4. This illustration clearly shows that higher values of σ substantially decrease the prevalence of snuffing, irregular, and regular smoking behaviors, highlighting the significant effect of smoking-related mortality on these categories.

In a system, the increase in natural death rate will decrease the population size. This is evidently captured in Figure 5. (i.e.) As natural death rate (β) increases, there is decreases in the overall population.

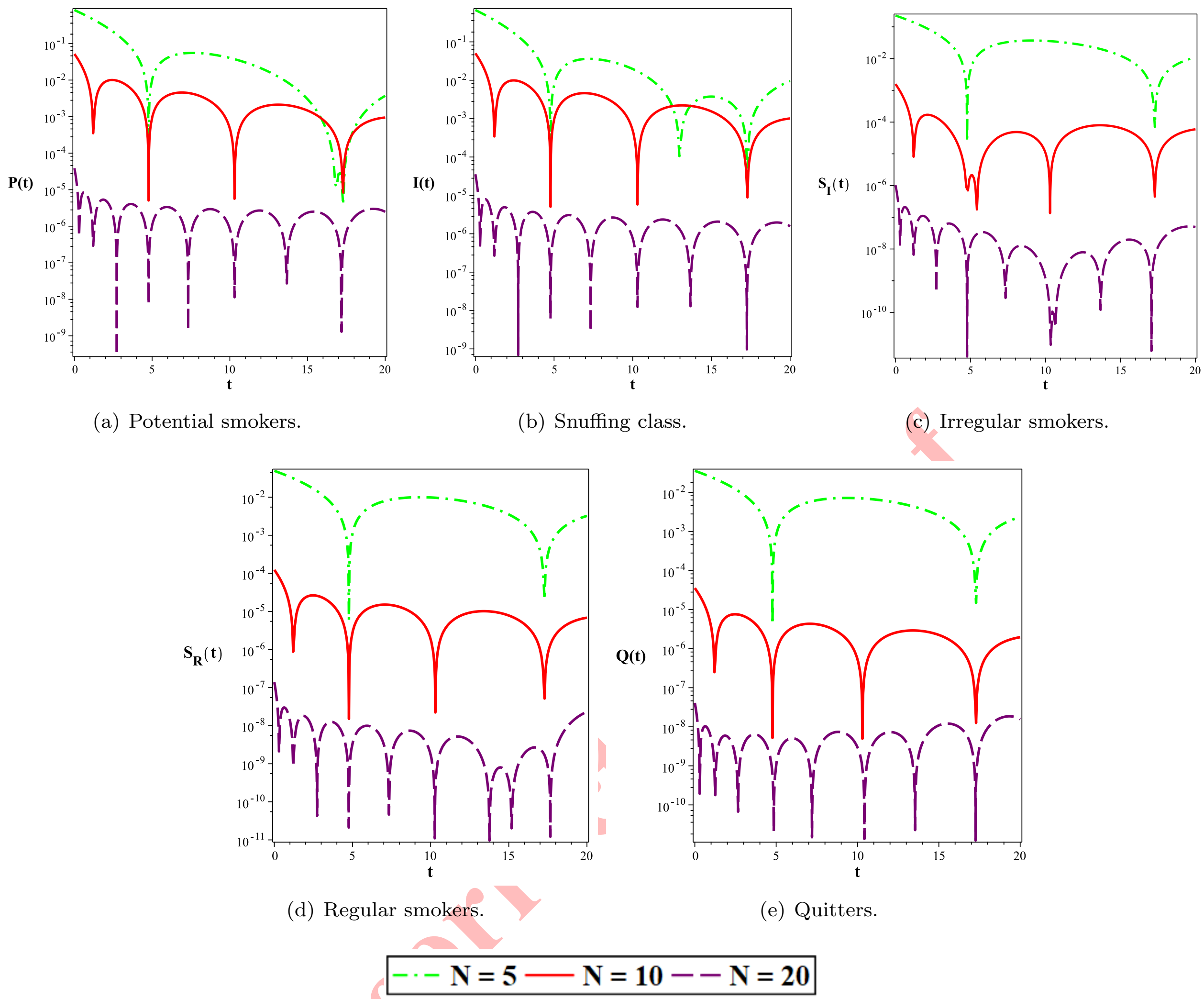

(a) Potential smokers. (b) Snuffing class. (c) Irregular smokers.

(d) Regular smokers. (e) Quitters.

FIGURE 2. Residual error for different values of N.

Figure 6 illustrates the influence of transmission rate (l_1) from potential smokers to snuffing class on five compartments. In a system, when the transmission rate increases, it increases the initiation of smoking among individuals thereby reducing the number of potential smokers. Thus, the potential smokers decrease when the transmission rate (l_1) increases. Consequently, this leads to an increase in the snuffing, irregular, regular smokers and quitters, as more individuals move into these categories.

The influence of the transmission rate (l_2) from the snuffing class to irregular smokers over the snuffing class, irregular and regular smokers are exhibited in Figure 7. It is observed from the figure that, as l_2 increases, the population of irregular and regular smokers increases whereas the population in the snuffing class decreases. This occurs because a higher transmission rate (l_2) encourages more people to start smoking, resulting in an increase in the number of individuals in the irregular and regular smokers and consequently decrease in the snuffing class.

Figure 8 highlights the impact of the transmission rate (l_3) from irregular to regular smokers over the smoker class. As the transmission rate (l_3) increases, the population of irregular smokers diminishes due to increased transmission of individuals into regular smokers from irregular smokers. This shift leads to a significant increase in the number of

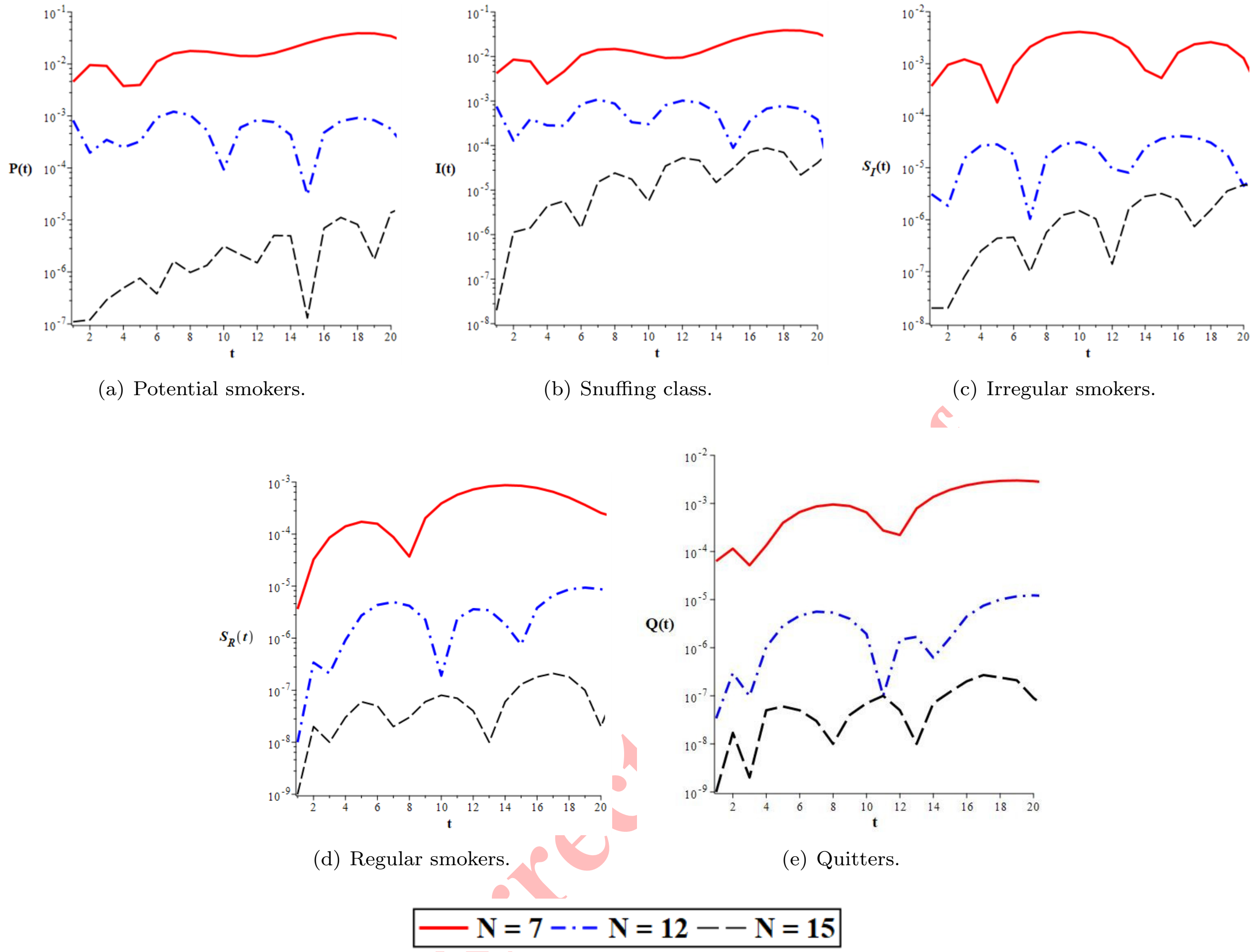

(a) Potential smokers. (b) Snuffing class. (c) Irregular smokers.

(d) Regular smokers. (e) Quitters.

FIGURE 3. Absolute error for different values of N.

regular smokers. The figure effectively illustrates the significant influence of l_3 on smoking behavior from irregular to regular smoking.

Figure 9 demonstrates the influence of the quit rate (α) over irregular, regular smokers, and quitters. This figure shows that as the quit rate (α) increases, the number of quitters rises which causes the population of both irregular and regular smokers to decrease. In a system, when both irregular and regular smokers stop smoking, the smoking population decreases, leaving an increase in the quitter population which is captured in Figure 9.

Figure 10 illustrates the effect of the recovery rate (γ) over $P(t), S_I(t), S_R(t)$ and $Q(t)$. As γ increases, individuals from the regular and irregular smokers revert to the potential smoker category. As a result, the number of potential smokers rises, while the number of irregular and regular smokers, and quitters decreases. This pattern indicates that a higher recovery rate promotes smoking cessation and reintegration into the susceptible population. The figure also highlights the significant impact of recovery rate variations on the overall dynamics of smoking behavior in the general population.

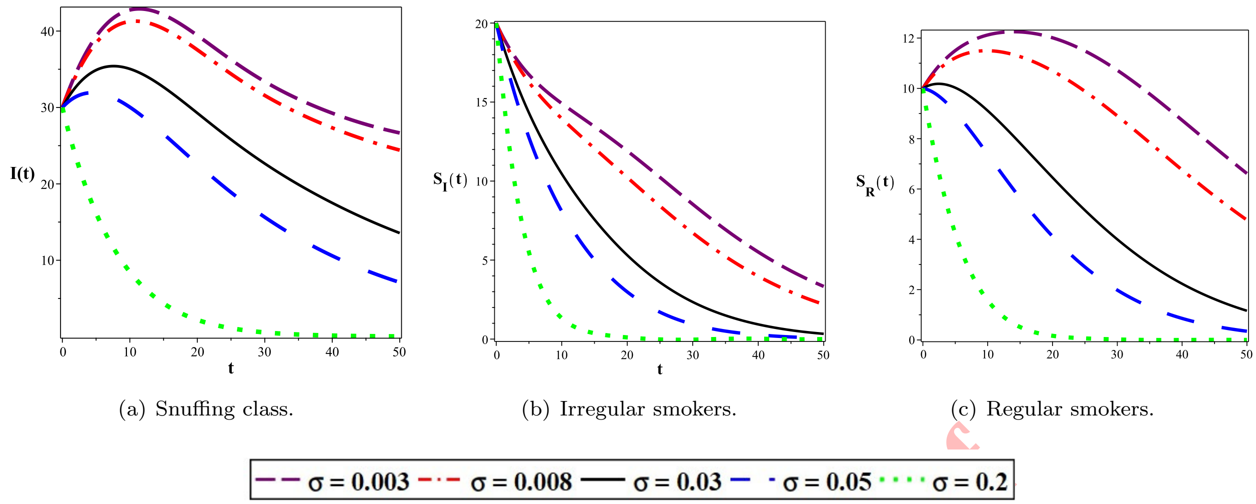

(a) Snuffing class. (b) Irregular smokers. (c) Regular smokers.

FIGURE 4. Influence of smoking related death rate (σ).

Figure 11–16 represents the contour plots for different combination of parameters at $t = 10$. The contour graph in Figure 11 illustrates the relationship between the death rate due to snuffing/smoking (σ) and transmission rate (l_1) on the snuffing, irregular, and regular smokers. It is inferred from the graph that the combined effect of high death and transmission rate decreases the population in both snuffing and smoker classes. This is because smokers are more likely to exit the system due to death, which leads to a decrease in the smoking class. Conversely, a high transmission rate coupled with a low death rate suggests an increased number of smokers across all three categories. This demonstrates that the interplay between transmission and death rates critically impacts the dynamics of smoking prevalence. Targeting these rates in public health interventions can effectively reduce smoking across different smoker categories.

Figure 12 examines the combined impact of two transmission rates, l_1 (from the potential smokers to snuffing class) and l_3 (from irregular smokers to regular smokers), on the populations of irregular and regular smokers. When both transmission rates l_1 and l_3 are high, the number of irregular smokers decreases and the number of regular smokers increases. This is because as l_3 increases, the rate at which irregular smokers develop a regular smoking habit, resulting in a notable rise in regular smoking and a decrease in irregular smoking. It can be noted that both irregular and regular smokers are influenced by l_3 compared to l_1 which is captured in contour plot Figure 12.

Figure 13 illustrates the combined effect of transmission rates l_2 (from the snuffing class to irregular smokers) and l_3 (from irregular smokers to regular smokers) over the irregular and regular smokers. When both transmission rates l_2 and l_3 are high, more individuals transmits from snuffing to irregular smoking and then to regular smoking, resulting in an increased number of regular smokers. Conversely, when both rates are low, fewer individuals move to regular smoking, leading to a reduced population of regular smokers. If the transmission rate l_2 is low and l_3 is high then the number of individuals move rapidly to regular smokers which leads to a decrease in irregular smokers which is captured in 13(a). Figure 13(b) demonstrates that an increase in $S_R(t)$ is associated with higher l_3 values. To effectively reduce the number of regular smokers, it is essential to lower l_3. The graph shows that by keeping l_3 below 0.04 and increasing l_2, we can raise the population of irregular smokers while reducing the conversion to regular smokers. This highlights the importance of controlling l_3 to mitigate the shift from irregular to regular smokers.

Figure 14 presents a contour graph depicting irregular and regular smokers based on the interaction between the transmission rate (l_1) and the recovery rate (γ). The figure reveals that a high transmission rate (l_1) combined with a low recovery rate (γ) leads to the highest number of irregular and regular smokers. Conversely, the combination

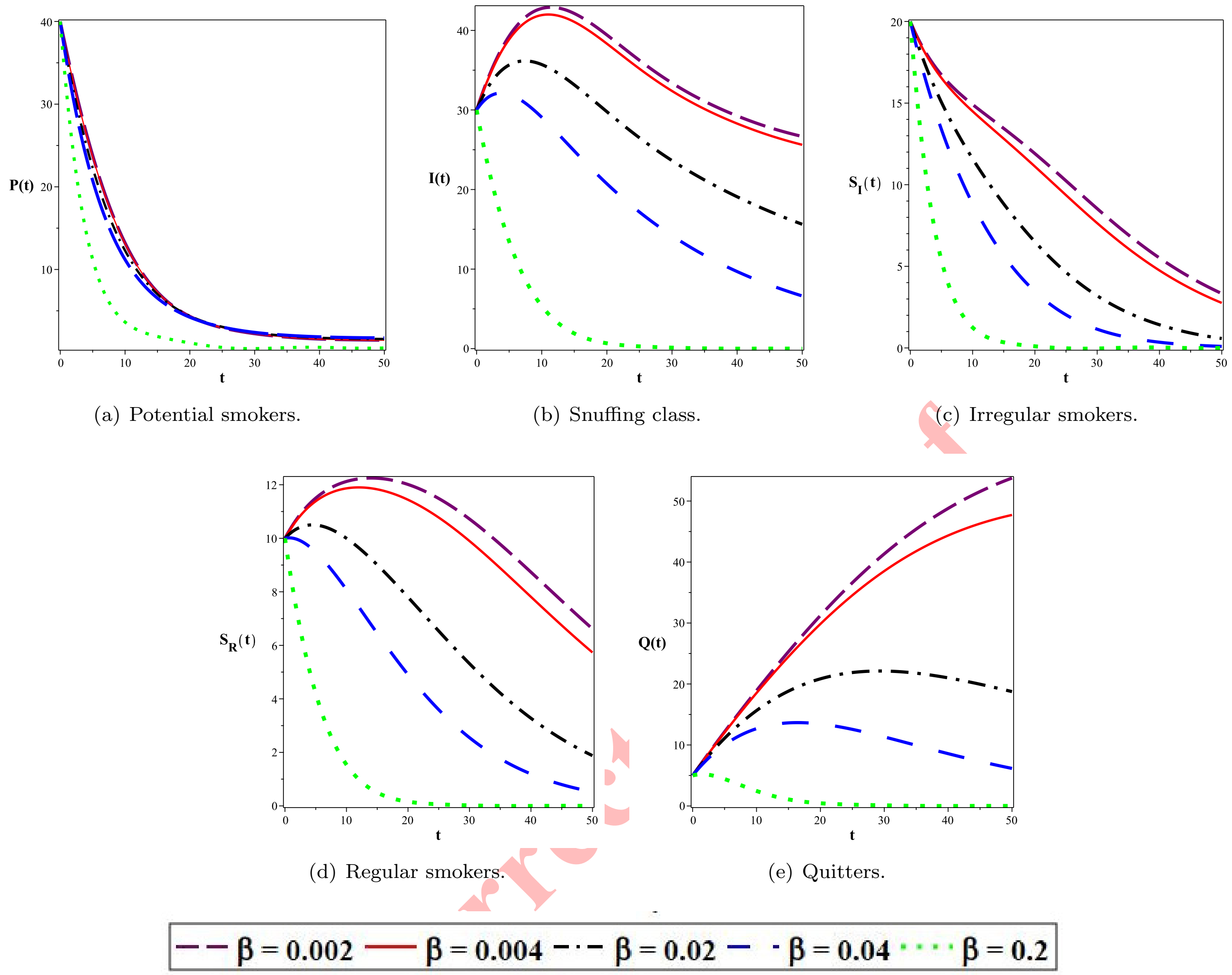

(a) Potential smokers. (b) Snuffing class. (c) Irregular smokers.

(d) Regular smokers. (e) Quitters.

Figure 5. Influence of natural death rate (β).

of low transmission rate (l_1) and high recovery rate (γ) lead to the lowest number of irregular and regular smokers. This is due to the highest influence of the transmission rate, which accelerates the growth of the smoking population. Conversely, as the recovery rate increases, individuals begin to recover from the smoking habit, leading to a decrease in the smoking population. To effectively reduce the number of smokers, it is essential to focus on strategies that reduce the transmission rate (l_1) and increase the recovery rate (γ). This combined approach will lead to a significant decrease in the proportions of smokers in the population over time.

Figure 15 presents a contour graph depicting the proportions of transmission rate (l_2) and recovery rate (γ) over irregular and regular smokers. The graph shows that a higher transmission rate (l_2) and a lower recovery rate (γ) yield an increased number of smokers as the higher transmission rate encourages more individuals to start smoking and a lower recovery rate hinders their ability to quit. Conversely, a lower transmission rate (l_2) and higher recovery rate (γ) lower the smoker population. It can be also observed from the figure that both irregular and regular smokers are influenced by the recovery rate than the transmission rate. That is, reducing l_2 and increasing γ can effectively lower

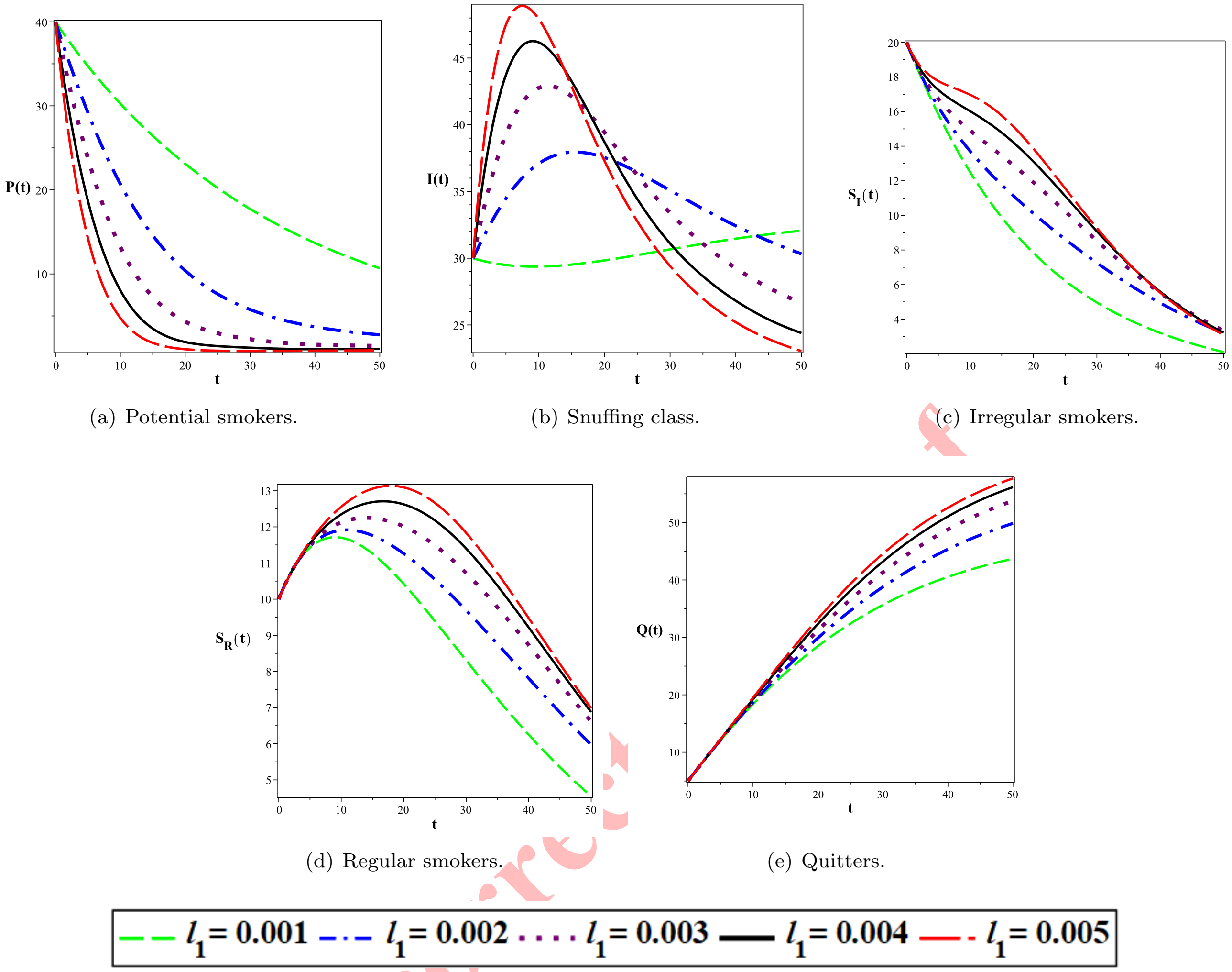

(a) Potential smokers. (b) Snuffing class. (c) Irregular smokers.

(d) Regular smokers. (e) Quitters.

FIGURE 6. Influence of transmission rate (l_1).

both irregular and regular smoking population over time. Therefore, strategies aimed at reducing the transmission rate and enhancing the recovery rate can significantly impact public health by decreasing the prevalence of smoking.

Figure 16 illustrates the influence of the combined parameters, such as the transmission rate (l_3) and the quit rate (α), on regular smokers. It can be noted that the population of regular smokers decreases to a greater extent for the same proportion of transmission and quit rate. For example, when l_3 and α are both increased from 0.1 to 0.3 in the same proportion, the corresponding population of regular smokers decreases by 83%. (i.e) The population is decreased from 9.56 to 1.58.

Precisely, Figure 11–16 suggests that boosting the recovery rate or quit rate and reducing the transmission rates can significantly decrease the number of smokers in the population. This underscores the importance of targeted interventions to improve these rates and effectively reduce smoking prevalence among individuals.

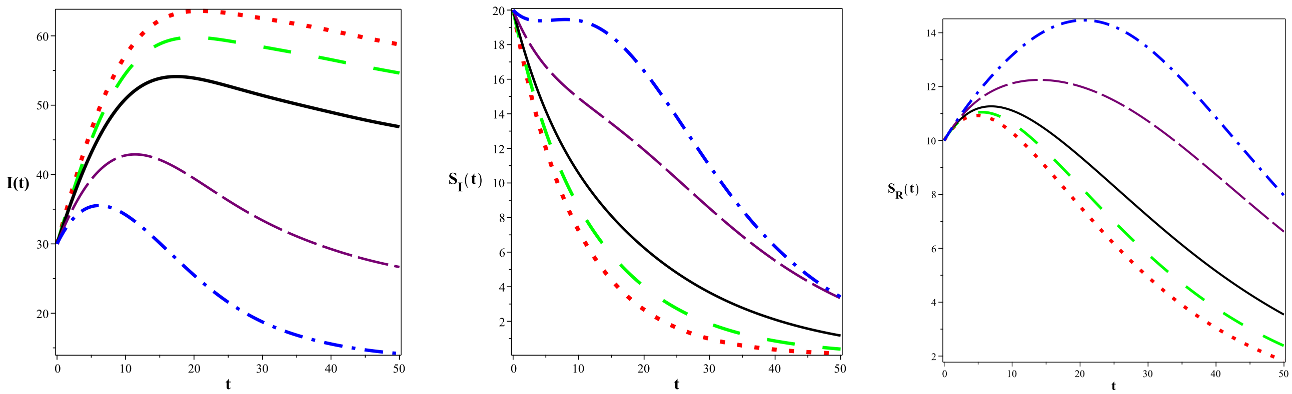

(a) Snuffing class. (b) Irregular smokers. (c) Regular smokers.

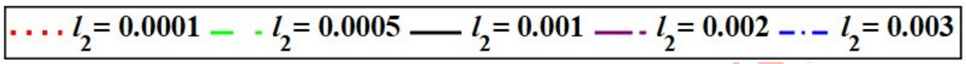

FIGURE 7. Influence of transmission rate (l_2).

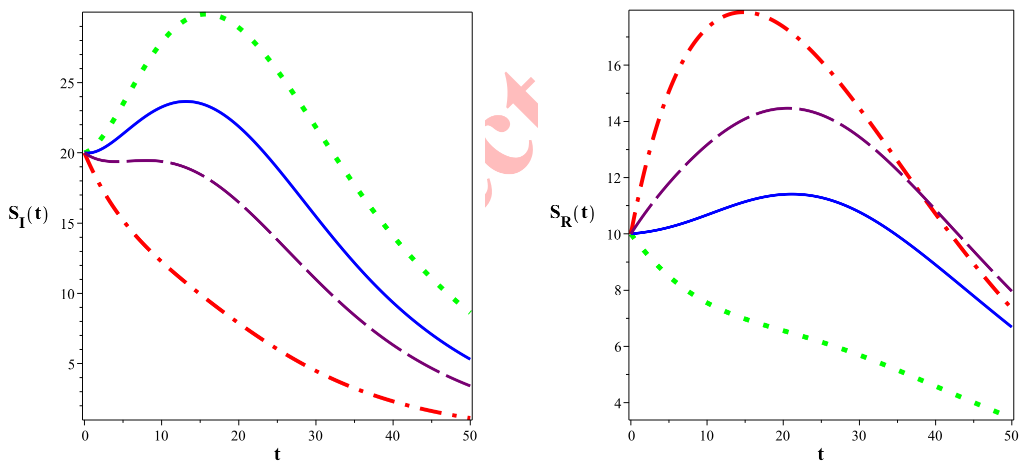

(a) Irregular smokers. (b) Regular smokers.

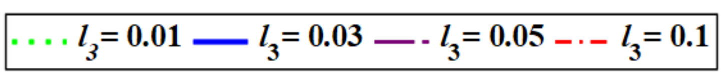

FIGURE 8. Inf1uence of transmission rate (l_3).

5. Conclusion

In this study, a five-compartment smoking model which is a system of non-linear differential equations is presented. Firstly, we modified a smoking model by adding various parameters, such as quit rate and recovery rate for irregular smokers and death rate for irregular and regular smokers. The key findings of the paper is discussed as follows:

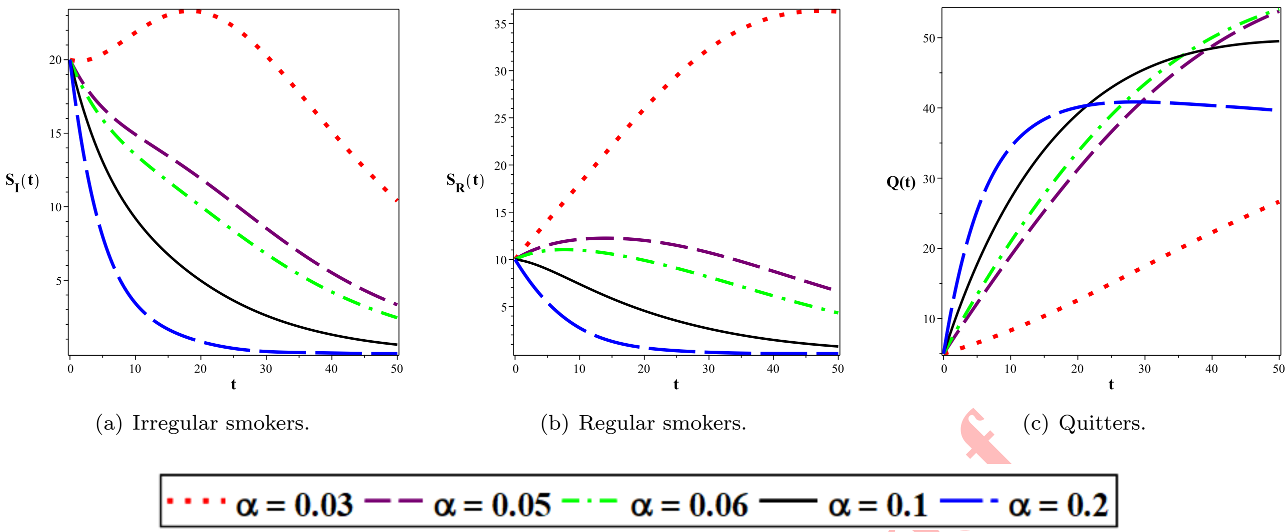

(a) Irregular smokers. (b) Regular smokers. (c) Quitters.

Figure 9. Influence of quit rate (α).

- The proposed model has been studied using the spectral collocation method with Chebyshev polynomials as basis function due to its low computational time and exponential convergence. This numerical approach has not been previously explored in the literature for these governing equations. The spectral collocation method is one of the best techniques for the smoking model.
- The residual error and the absolute error are depicted in the form of graphs. The residual error analysis indicates that as N increases, the residual error decreases, that is, the solution begins to converge. In the case of absolute error, the present method results were compared with those of the RK-4 method and found that the accuracy increases to $O(10^{-7})$ as N increases from 7 to 15.
- The influence of various model parameters such as transmission rate (l_1, l_2, l_3), death rate (β, σ), recovery rate (γ) and quit rate (α) of the proposed model has been captured as follows:
  - As the natural death rate (β) increases, there is a decrease in the total population. This decrease suggests a reduction in population size, which could potentially lead to a decrease in smoking incidence as there would be fewer potential individuals who might start smoking.
  - As σ (death rate due to snuffing/smoking) increases, the population in the snuffing class, irregular and regular smokers decreases. It underscores the potential impact of mortality risks associated with smoking on reducing smoking prevalence and encouraging individuals to quit or avoid smoking altogether.
  - As the transmission rate l_1 (potential smokers to snuffing class) increases, individuals from the potential smokers start to smoke which leads to a decrease in $P(t)$ and an increase in all other compartments.
  - As the transmission rate l_2 (from the snuffing class to irregular smokers) increases, individuals transmitted from the snuffing to the irregular smoking class more rapidly. This results in a decrease in the number of individuals in the snuffing class, while there is an increase in the number of irregular and regular smokers, as well as quitters.
  - As the transmission rate l_3 (from the irregular smokers to regular smokers) increases, more individuals transmitted from irregular to regular smoking class. Thus, there is a decrease in irregular smokers and an increase in regular smokers.
  - As the quit rate (α) increases, there is an increase in the number of quitters and a decrease in both irregular and regular smokers. This suggests that the quit rate is a crucial determinant in reducing smoking prevalence.

   – As the recovery rate (γ) increases, it leads to a decrease in both irregular and regular smokers, which suggests that the recovery rate is a critical factor in reducing smoking prevalence.

- Contour plots were used to analyse the combined effects of various parameter interactions on the smoking dynamics. Our results demonstrated that the interplay between these parameters has a substantial impact on smoking behaviors. Specifically,
   – A combination of high transmission rate and the death due to snuffing/smoking parameter decreases the population in snuffing and other smoker compartments.
   – A combination of high transmission rates l_1 and l_3 leads to a decrease in irregular smokers and an increase in regular smokers, as l_3 drives the transmission from irregular to regular smoking.
   – A combination of high l_2 and low l_3 leads to a decrease in regular smokers and an increase in irregular smokers. Increasing l_2 while keeping l_3 low will boost the irregular smokers and reduce their transition to regular smoking. Controlling l_3 is crucial for managing the regular smoker population.

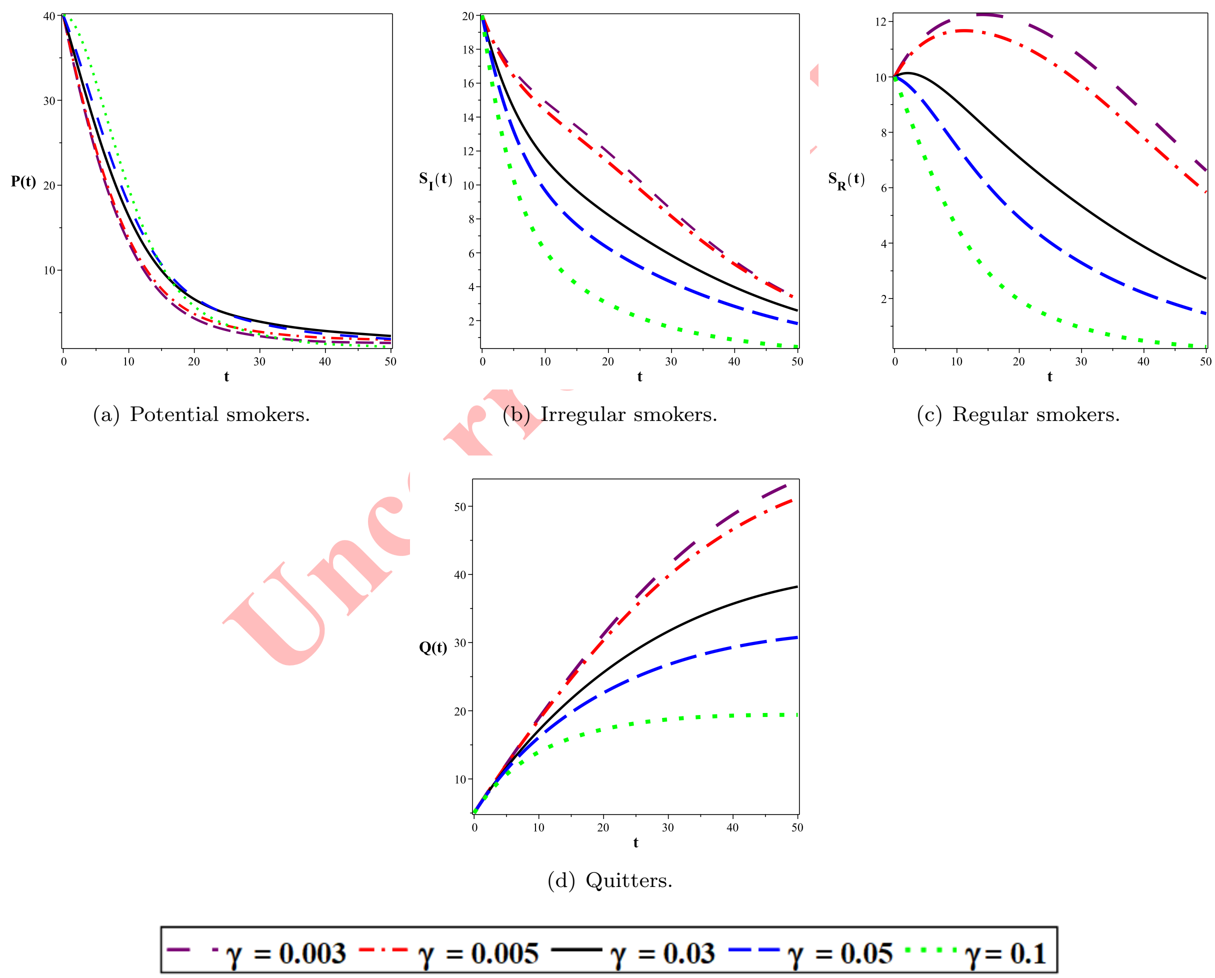

(a) Potential smokers. (b) Irregular smokers. (c) Regular smokers.

(d) Quitters.

FIGURE 10. Influence of recovery rate (γ).

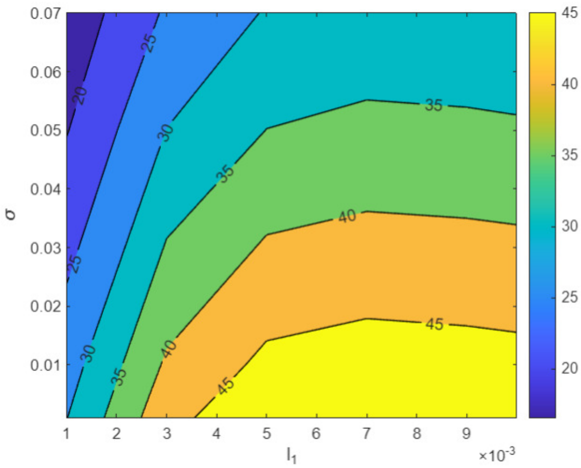

(a) Snuffing class.

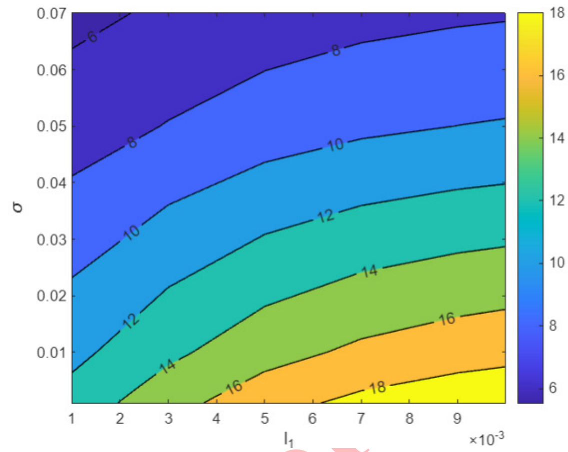

(b) Irregular smokers.

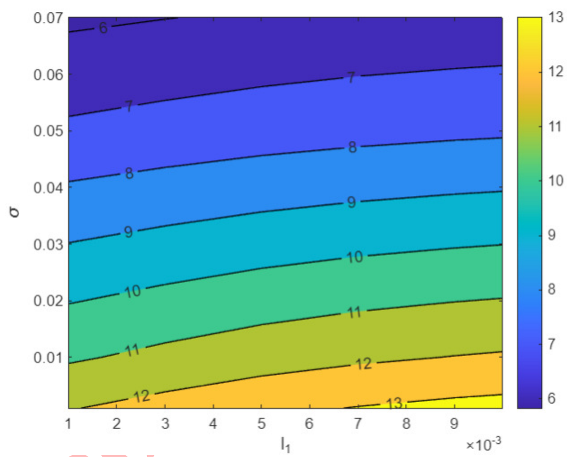

(c) Regular smokers.

FIGURE 11. Effects of the transmission rate (l_1) and the death due to smoking (σ).

- The combination of high transmission rates (l_1) and low recovery rate (γ) results in an increase in the smoker class, while low transmission rates and high recovery rate lead to a decrease in the smoker class. This pattern is also observed with the interplay between l_2 and γ.
- The combination of high transmission rate (l_3) and low quit rate (α) increase the regular smokers. Conversely, the low transmission rate (l_3) and high quit rate (α) reduce the regular smokers. That is, higher quit rates contributing to a reduction in the number of smokers.

- Our analysis identifies several critical intervention points for controlling smoking behavior. High transmission rates (l_1 and l_3) should be targeted to prevent the increase of regular smokers. Reducing l_1 can help in decreasing the transmission from potential smokers to smoking categories, while managing l_3 is crucial for controlling the shift from irregular to regular smoking. Enhancing the recovery rate (γ) can significantly reduce the overall number of smokers, especially when transmission rates are high. Finally, promoting higher quit rates (α) is also vital for decreasing regular smoker prevalence. Thus, this study help us to analysis the impact of the different parameters on susceptible, snuffing, irregular, regular and quitter individuals of the smoking model. These interventions, focused on reducing transmission rates, increasing recovery rates, and boosting quit rates, are essential for effective smoking cessation programs.

In conclusion, these findings offer practical guidance for designing targeted interventions to reduce smoking. The figures and additional factors incorporated into the model enhance its ability to capture the complexities of smoking behavior dynamics. This analysis supports the development of effective strategies to reduce smoking rates and improve health outcomes.

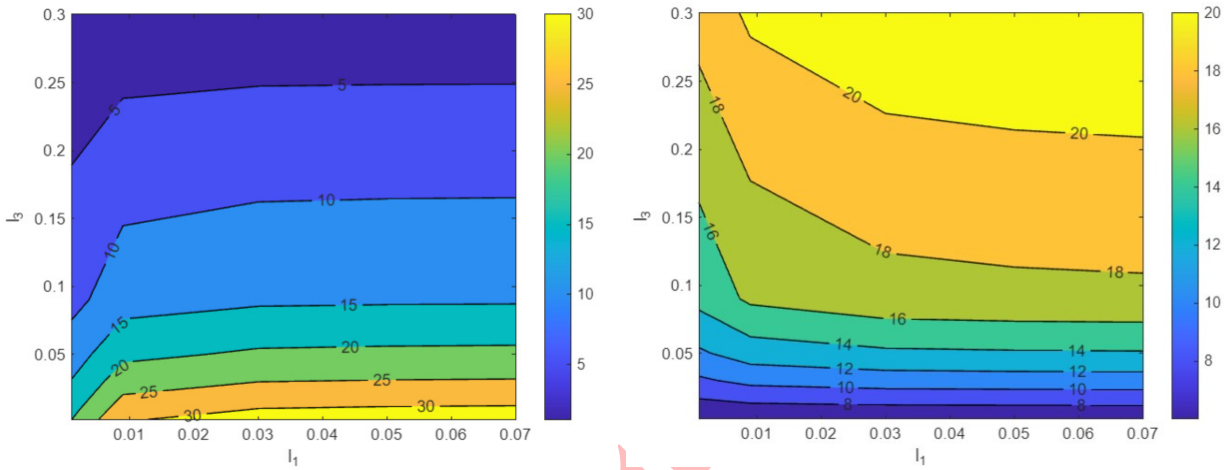

(a) Irregular smokers. (b) Regular smokers.

FIGURE 12. Effects of the transmission rate (l_1) and the transmission rate (l_3).

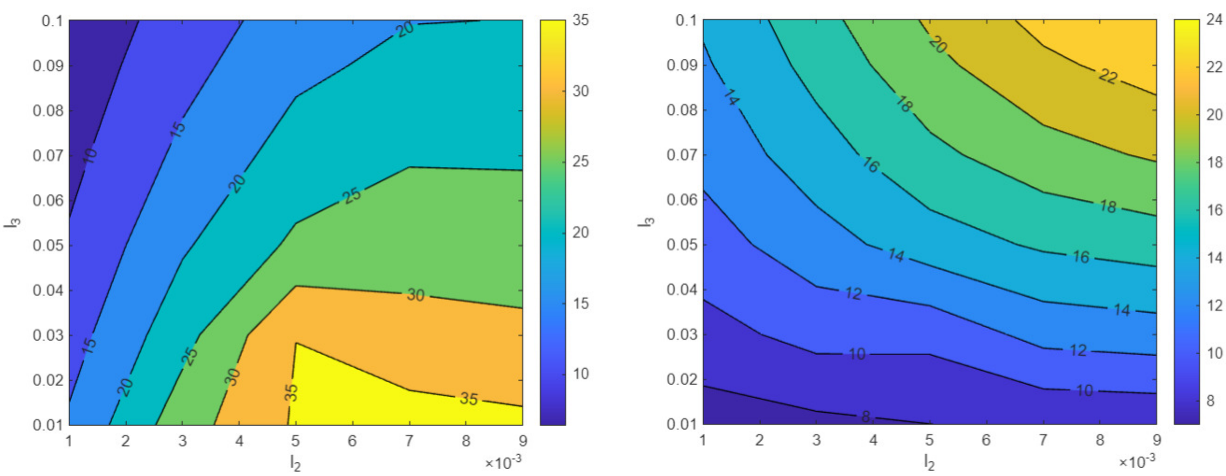

(a) Irregular smokers. (b) Regular smokers.

FIGURE 13. Effects of the transmission rate (l_2) and the transmission rate (l_3).

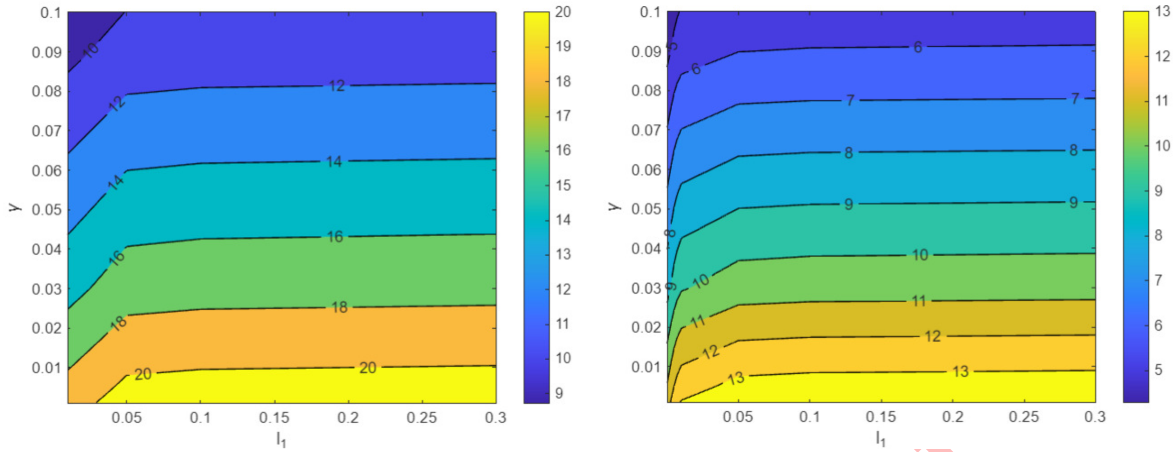

(a) Irregular smokers.

(b) Regular smokers.

FIGURE 14. Effects of the transmission rate (l_1) and recovery rate (γ).

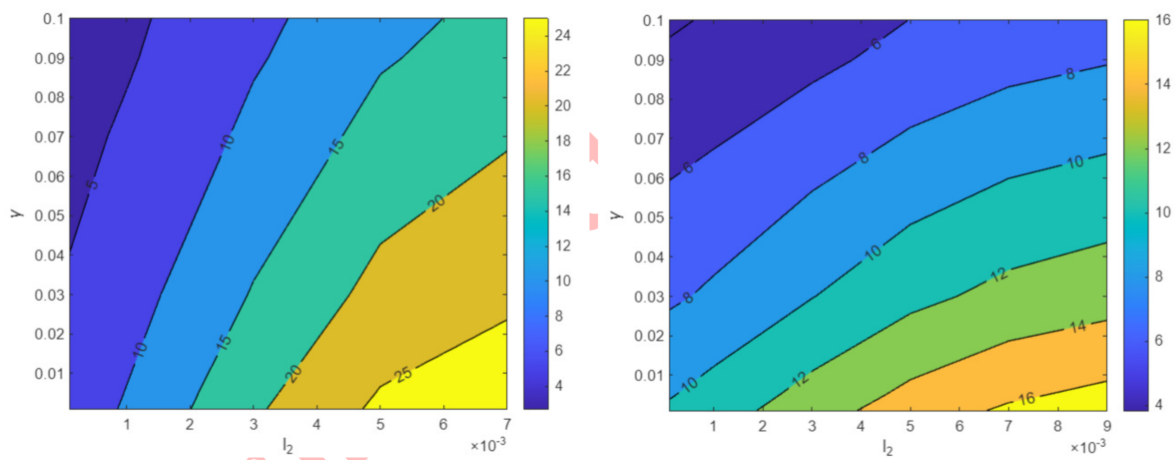

(a) Irregular smokers.

(b) Regular smokers.

FIGURE 15. Effects of the transmission rate (l_2) and recovery rate (γ).

Acknowledgment

Funding. No funding is involved.

Conflict of interest. The authors have no conflict of interest to be declared here.

Acknowledgement. We sincerely appreciate the esteemed reviewers and the dedicated editorial team for their meticulous evaluation, insightful feedback, and constructive suggestions on our manuscript.

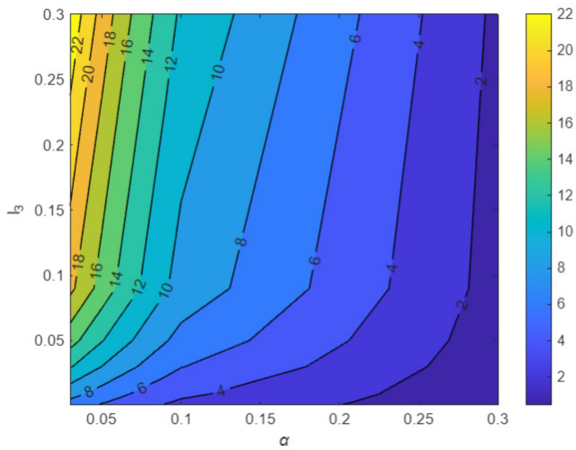

(a) Regular smokers.

FIGURE 16. Effects of the transmission rate (l_3) and quit rate (α).

REFERENCES

[1] R. M. Anderson and R.M. May, *Population biology of infectious diseases: Part I. Nature*, *280*(5721) (1979), 361-7.

[2] R. M. Anderson and R.M. May, *Infectious diseases of humans: dynamics and control*, Oxford University Press, (1991).

[3] R. M. Anderson, *Discussion: the Kermack-McKendrick epidemic threshold theorem*, Bulletin of Mathematical Biology, *53* (1991), 1-32.

[4] Z. Alkhudhari, S. Al-Sheikh, and S. Al-Tuwairqi, *Global dynamics of a mathematical model on smoking*, International Scholarly Research Notices, *1* (2014), 847075.

[5] E. Alzahrani and A. Zeb, *Stability analysis and prevention strategies of tobacco smoking model*, Boundary Value Problems, (2020), 1-3.

[6] A. A. Alshareef and H. A. Batar, *Stability analysis of chain, mild and passive smoking model*, American Journal of Computational Mathematics, *10*(1) (2020), 31.

[7] A. U. Awan, A. Sharif, K. A. Abro, M. Ozair, and T. Hussain, *Dynamical aspects of smoking model with cravings to smoke*, Nonlinear Engineering, *10*(1) (2021), 91-108.

[8] L. Bednarova, Z. Simkova, A. Behunova, and A. Wozny, *How does the Excise Tax Affect Secondhand Smokers and the Health Consequences of such Addiction?*, Addictology/Adiktologie, *2* (2023).

[9] C. Cesarano, *Generalized Chebyshev polynomials*, Hacettepe Journal of Mathematics and Statistics, *43*(5) (2014), 731-740.

[10] H. Choi, I. Jung, and Y. Kang, *Giving up smoking dynamic on adolescent nicotine dependence: a mathematical modeling approach*, In: KSIAM 2011 Spring Conference, Daejeon, Korea, (2011).

[11] Y. Chakir, *Semi-analytical method for solving a model of the evolution of smoking habit using global rational approximants*, International Journal of Dynamics and Control, *12*(6) (2024), 1717-1727.

[12] G. Dattoli and C. Cesarano, *On a new family of Hermite polynomials associated to parabolic cylinder functions*, Applied Mathematics and Computation, *141*(1) (2003), 143-149.

[13] Q. Din, M. Ozair, T. Hussain, and U. Saeed, *Qualitative behavior of a smoking model*, Advances in Difference Equations, (2016), 1-2.

[14] D. Gottlieb and S. A. Orszag, *Numerical analysis of spectral methods: theory and applications*, Society for Industrial and Applied Mathematics, (1977).

[15] C. C. Garsow, G. J. Salivia, and A. R. Herrera, *Mathematical Models for the Dynamics of Tobacco use, recovery and relapse*, Technical Report Series BU-1505-M. UK: Cornell University, (2000).

[16] I. Goldenberg, M. Jonas, A. Tenenbaum, V. Boyko, S. Matetzky, A. Shotan, S. Behar, and H. Reicher-Reiss, Bezafibrate Infarction Prevention Study Group, *Current smoking, smoking cessation, and the risk of sudden cardiac death in patients with coronary artery disease*, Archives of internal medicine, *163*(19) (2003), 2301-2305.

[17] O. K. Ham, *Stages and processes of smoking cessation among adolescents*, Western Journal of Nursing Research, *29*(3) (2007), 301-315.

[18] T. Hussain, A. U. Awan, K. A. Abro, M. Ozair, and M. Manzoor, *A mathematical and parametric study of epidemiological smoking model: a deterministic stability and optimality for solutions*, European Physical Journal Plus, *136* (2021), 1-23.

[19] M. M. Khader and A. H. Tedjani, *Numerical simulation for the fractional-order smoking model using a spectral collocation method based on the Gegenbauer wavelet polynomials*, Journal of Applied Analysis and Computation, *14*(2) (2024), 847-863.

[20] S. Kumbinarasaiah and R. Yeshwanth, *A numerical study of the evolution of smoking habit model through Haar wavelet technique*, International Journal of Dynamics and Control, (2024), 1-19.

[21] A. L. Mojeeb and I. K. Adu, *Modelling the dynamics of smoking epidemic*, Journal of Advances in Mathematics and Computer Science, *25*(5) (2017), 1-19.

[22] O. Sharomi and A. B. Gumel, *Curtailing smoking dynamics a mathematical modeling approach*, Applied Mathematics and Computation, *195(2)*(2008), 475-499.

[23] J. M. Samet, *Tobacco smoking: the leading cause of preventable disease worldwide*, Thoracic Surgery Clinics, *23*(2) (2013), 103-12.

[24] N. H. Shah, F. A. Thakkar, and B. M. Yeolekar, *Stability analysis of tuberculosis due to smoking*, Int J Innov Sci Res Technol, *3*(1) (2018), 230-7.

[25] L. N. Trefethen, *Spectral methods in MATLAB*, Society for industrial and applied mathematics, (2000).

[26] S. Thirumalai, R. Seshadri, and S. Yuzbasi, *Population dynamics between a prey and a predator using spectral collocation method*, International Journal of Biomathematics, *12*(05) (2019), 1950049.

[27] S. Thirumalai, R. Seshadri, and S. Yuzbasi, *On the solution of the human immunodeficiency virus (HIV) infection model using spectral collocation method*, International Journal of Biomathematics, *14*(02) (2021), 2050074.

[28] S. Thirumalai, R. Seshadri, and S. Yuzbasi, *Spectral collocation method based on special functins for solving nonlinear high-order pantograph equations*, Computational Methods for Differential Equations, *11*(3) (2023), 589-604.

[29] G. Ur Rahman, R. P. Agarwal, and Q. Din, *Mathematical analysis of giving up smoking model via harmonic mean type incidence rate*, Applied Mathematics and Computation, *354* (2019), 128-48.

[30] World Health Organization. *Tobacco control for sustainable development*, World Health Organization, Regional Office for South-East Asia, (2017).

[31] R. West, *Tobacco smoking: Health impact, prevalence, correlates and interventions*, Psychology and health, *32*(8) (2017), 1018-1036.

[32] G. Zaman, *Qualitative behavior of giving up smoking models*, Bulletin of the Malaysian Mathematical Sciences Society, Second Series *34*(2) (2011), 403-415.

[33] G. Zaman, *Optimal campaign in the smoking dynamics*, Computational and Mathematical Methods in Medicine, *1* (2011), 163834.

[34] A. Zeb, G. Zaman, and S. Momani, *Square-root dynamics of a giving up smoking model*, Applied Mathematical Modelling, *37*(7) (2013), 5326-34.

[35] Z. Zhang, J. Zou, R.K. Upadhyay, and A. Pratap, *Stability and Hopf bifurcation analysis of a delayed tobacco smoking model containing snuffing class*, Advances in Difference Equations, *349* (2020), 1-19 .

[36] A. Zeb and A. Alzahrani, *Non-standard finite difference scheme and analysis of smoking model with reversion class*, Results in Physics, *21* (2021), 103785.